*minerals*

MDPI

*Article*

# Comparative Study on Refractory Gold Concentrate Kinetics and Mechanisms by Pilot Scale Batch and Continuous Bio-Oxidation

**Zhong-Sheng Huang [1,2,3,*] and Tian-Zu Yang [1]**

[1] School of Metallurgy and Environment, Central South University, Changsha 410083, China; tianzuyang@csu.edu.cn
[2] State Key Laboratory of Comprehensive Utilization of Low-Grade Refractory Gold Ores, Xiamen 361000, China
[3] Zijin Mining Group Company Limited, Longyan 364200, China
* Correspondence: zshuang@csu.edu.cn

**Abstract:** Most studies conducted have focused on the pulp density, $Fe^{3+}$ concentration and sulfuric acid concentration, etc., of bio-oxidation, and few have reported on the influence of different bio-oxidation methods on kinetics. In this study, a comparative investigation on refractory gold concentrate by batch and continuous bio-oxidation was conducted, with the purpose of revealing the kinetics influence. The results showed that improving the removal rates of the gold-bearing pyrite ($FeS_2$) and arsenopyrite (FeAsS) yielded the best results for increasing gold recovery. The removal rates of S, Fe and relative gold recovery linearly increased when compared to the second-order equation increase of the As removal rate in both batch and continuous bio-oxidation processes. The removal kinetics of S and Fe by continuous bio-oxidation was 12.02% and 12.17% per 24 h day, approximately 86.64% and 51.18% higher than batch bio-oxidation, respectively. The higher removal kinetics of continuous bio-oxidation resulted from a stepwise increase in microbe growth, a larger population and higher dissolved $Fe^{3+}$ and $H_2SO_4$ concentration compared to a linear increase by batch bio-oxidation. The cyanidation gold recovery was as high as 94.71% after seven days of continuous bio-oxidation, with the gold concentrate sulfur removal rates of 83.83%; similar results will be achieved after 13 days by batch bio-oxidation. The 16sRNA sequencing showed seven more microbe cultures in the initial residue than Acid Mine Drainage (AMD) at genus level. The quantitative real-time Polymerase Chain Reaction (PCR) test showed the four main functional average microbe populations of *Acidithiobacillus*, *Leptospirillum*, *Ferroplasma* and *Sulfobacillus* in continuous bio-oxidation residue as $1.08 \times 10^3$ higher than in solution. The multi-microbes used in this study have higher bio-oxidation activity and performance in a highly acidic environment since some archaea co-exist and co-contribute.

**Keywords:** refractory gold concentrate; continuous bio-oxidation; batch bio-oxidation; kinetics and mechanism; multi-microbes



**Citation:** Huang, Z.-S.; Yang, T.-Z. Comparative Study on Refractory Gold Concentrate Kinetics and Mechanisms by Pilot Scale Batch and Continuous Bio-Oxidation. *Minerals* **2021**, *11*, 1343. https://doi.org/10.3390/min11121343

Academic Editors: Jean-François Blais, Hongbo Zhao, Jiushuai Deng and Abhilash

Received: 15 October 2021
Accepted: 26 November 2021
Published: 29 November 2021



## 1. Introduction

Approximately one-third of the gold deposits in the world are refractory gold ores [1,2]. Roasting [3], pressure oxygen oxidation [4], bio-oxidation [5] and chemical oxidation [6,7] are the commercial pretreatment technologies normally used to improve gold recovery before cyanidation from refractory gold ores.

The roasting oxidation process is accomplished with heavy pollution and limited gold recovery, with 30% sulfide sulfur as the standard maximum content requirement in refractory gold concentrate. Pressure oxidation gold recovery usually yields higher outputs than any other oxidation techniques; however, only a few process plants are operational globally because of its high investment cost, and complex operating process. Pressure

oxygen oxidation requires a maximum of 20% sulfide sulfur in concentrate. The first refractory gold concentrate pressure oxygen oxidation plant was not established in China until 2016 by Shuiyindong Gold Mine, a wholly subsidiary company of Zijin Mining Group Co., Ltd in Guizhou province. Chemical oxidation was one of the technologies used in high gold content and low sulfide sulfur refractory gold ore; with oxygen, nitric acid, and sodium hydroxide as reductants and oxidants.

Bio-oxidation has been widely used in the gold recovery of refractory gold concentrate due to its environmentally benign, lower energy costs, smaller carbon footprint and effectiveness [8]. Currently, more than 20 bio-oxidation plants are operational worldwide. The first commercial bio-oxidation plant was established at Fairview mine in 1986 by BIOX technology [9], followed by others primarily located in Australia, China, Brazil, Ghana, Peru, and Russia. They produce approximately 5% of the total mine gold by bio-oxidation process [10]. Presently, research in this field is focused on improving bio-oxidation kinetics, shortening bio-oxidation time, or extending the limit of sulfide sulfur and arsenic content in the bio-oxidation concentrate. However, the previous focus areas were pulp density, $Fe^{3+}$ concentration, temperature, oxidation-reduction potential (ORP), sulfuric acid concentration on the bio-oxidation rate and kinetics [11–13]. Hence, it is difficult to obtain a unified standard because of the differences in experimental reactors, methods or bacteria, etc. There are also many conflicting or contradictory research results, because most of this research was conducted in small-scale laboratory reactors with different reactor types [14,15]. These studies were completed by small-scale laboratory batch bio-oxidation [16], with few comparative studies on batch and continuous bio-oxidation being reported. Secondly, many studies focused on single microbe culture bio-oxidation [17,18] but not multi-microbes, relative microbe composition, and population trend changes in the bio-oxidation process [19,20]. Finally, only a few bio-oxidation studies of high sulfur sulfide refractory gold concentrate were reported.

Chandraprabha [21] studied the bio-oxidation of refractory gold concentrate with sulfur content 29.25%, the results showed that the bio-oxidation rate was only 35% under the 10% pulp density and 60 days bio-oxidation with a wild strain of *Thiobacillus ferrooxidans*. A gold extraction efficiency of 90% would need 40 days of bio-oxidation even when the pulp density is progressively increased from 2 to 10%. Similar long bio-oxidation times and gold recovery results were also found in other research [22]. Hansford [23] investigated the kinetics of refractory gold concentrate by batch and continuous bio-oxidation, but the results showed that the pyrite bio-oxidation rate by batch bio-oxidation was close to those obtained from continuous bio-oxidation. However, the results achieved could not accurately reflect the true kinetics of batch and continuous bio-oxidation processes since the unusual single-stage continuous bioreactor process was adopted in this experiment.

This study compares kinetics and mechanisms of high sulfur sulfide and arsenic double refractory gold concentrate by batch and continuous bio-oxidation processes. An investigation on the removal rates and kinetics of S, Fe, and As from gold concentrate, as well as the variance in the dissolved concentration of Fe, $H_2SO_4$ and As were compared by batch and continuous bio-oxidation processes. In addition, the different microbe structures and populations during bio-oxidation were revealed.

## 2. Materials and Methods

### *2.1. Samples of Gold Concentrates*

The refractory gold concentrates used for these investigations were obtained from a gold mine process plant of Zijin Mining Group Co., Ltd. The particle size was 90%−0.074 mm. As shown in Tables 1 and 2, the sulfur and arsenic content were 38.42 and 2.10%, respectively, with sulfide sulfur accounting for 99.92% of the total sulfur. The gold enclosed by sulfide was 62.21%, in comparison to 32.89% of free gold, 4.89% of gold enclosed in oxides and sulfates and 0.44% of gold enclosed in silicate (Table 3). The enclosed gold was in the form of electrum. The pyrite ($FeS_2$) and arsenopyrite (FeAsS) contents were 73.1 and 3.2%, respectively, as compared to gangue sericite and quartz, which yielded 11.8% and 8.72%,

respectively. This is usually a typical trend between high sulfur and arsenic refractory gold concentrate in comparison with standard refractory concentrate. The chemical composition of the refractory gold concentrate is illustrated in Table 1. Sulfur and gold chemical phase compositions are shown in Tables 2 and 3, respectively. MLA (mineral liberation analyzer) mineral composition and mineralography analysis results are depicted in Figures 1 and 2, respectively. The size of free gold and gold enclosed by sulfide was as fine as −10 μm and −5 μm, respectively. The gold content in electrum enclosed by pyrite was higher than gold enclosed by arsenopyrite and quartz.

**Table 1.** Elemental analyses of the gold concentrate samples.

| Element | Au * | As | S | Fe | $SiO_2$ | MgO | Ag * | $Al_2O_3$ |
|---|---|---|---|---|---|---|---|---|
| wt.% | 26.96 | 2.10 | 38.42 | 35.16 | 15.10 | 0.68 | 20.4 | 3.68 |
| Element | Total C | $C_{organic}$ | Zn | Cr | CaO | Cu | Cd | Pb |
| wt.% | 0.66 | 0.30 | 0.15 | 0.053 | 0.64 | 0.063 | <0.01 | 0.11 |

* Au and Ag contents being g/t.

**Table 2.** Sulfur phases in the gold concentrate samples.

| Items | Sulfate Sulfur | Sulfide Sulfur | Other Sulfurs | Total S |
|---|---|---|---|---|
| Content/% | 0.03 | 37.82 | <0.0005 | 38.42 |
| Percentage/% | 0.08 | 99.92 | 0.00 | 100.00 |

**Table 3.** Gold chemical phase of gold concentrate samples.

| Items | Free Au | Au Enclosed by Oxide and Sulfate | Au Enclosed by Sulfide | Au Enclosed by Silicate | Total Au |
|---|---|---|---|---|---|
| Content/% | 8.73 | 1.19 | 16.51 | 0.11 | 26.54 |
| Percentage/% | 32.89 | 4.48 | 62.21 | 0.41 | 100.00 |

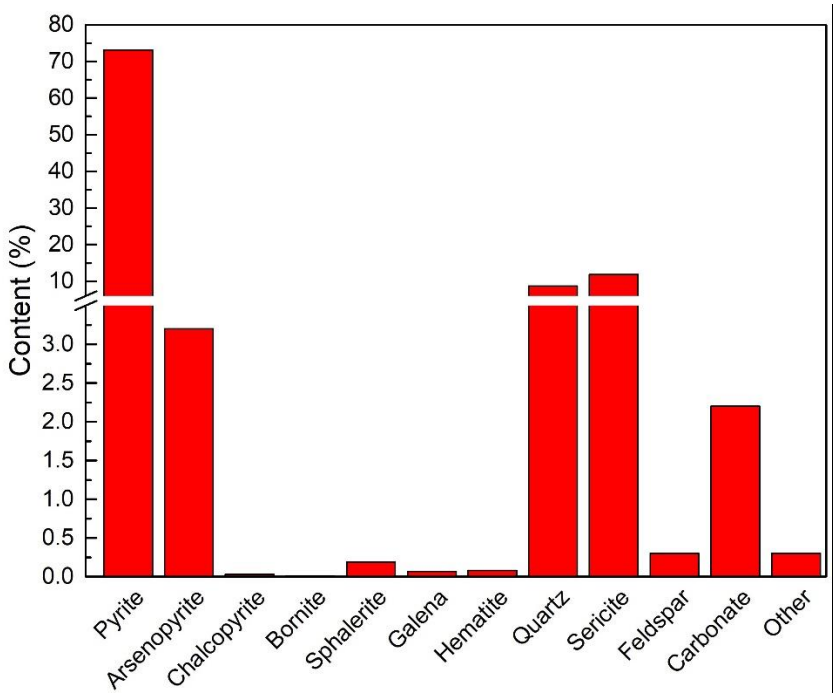


**Figure 1.** Mineral composition in refractory gold concentrate.

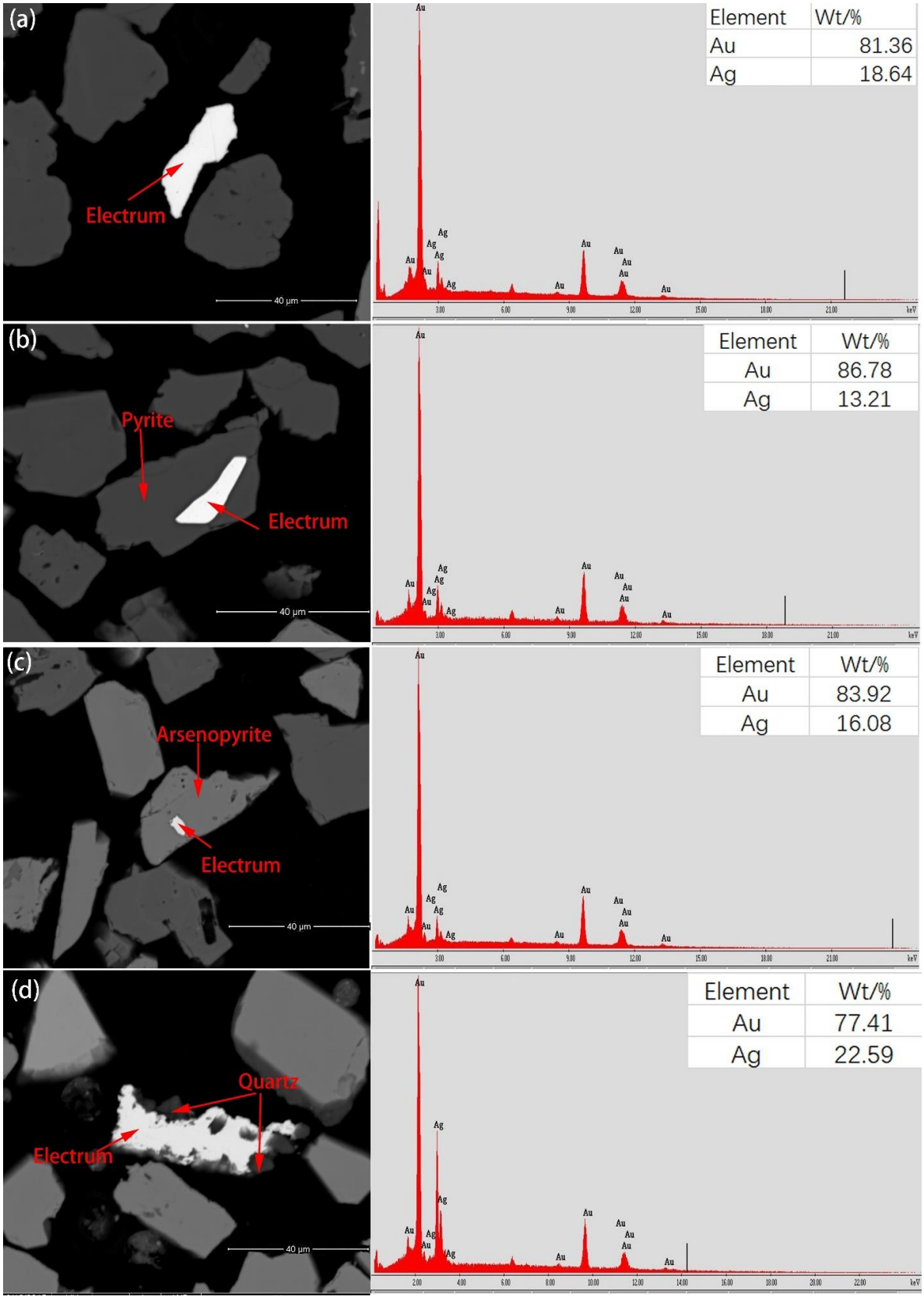


**Figure 2.** Micrographs of (**a**) free electrum, (**b**) electrum enclosed by pyrite, (**c**) electrum enclosed by arsenopyrite and (**d**) electrum enclosed by quartz.

### 2.2. Microbes and Growth Media

The microbes used for this test were acquired from waste acid residue and AMD (acid mine drainage) of Zijinshan Gold and Copper Mine, which is located at Fujian, China. These microbes were tamed in 9K medium (3.0 g/L $(NH_4)_2SO_4$, 0.1 g/L KCl, 0.5 g/L $K_2HPO_4$, 0.5 g/L $MgSO_4 \cdot 7H_2O$, 0.01 g/L Ca $(NO_3)_2$) for 3 months initially, and were subsequently tamed through gold concentrate slurry density, ion concentration and temperature gradients.

### 2.3. Methods

Batch bio-oxidation procedure: Batch bio-oxidation was conducted in 6 individual 200 L stainless steel tanks tandem to each other, having 30 kg gold concentrate, 180 L iron-free 9K medium and 10% cell suspension (15% pulp density). The test was conducted at initial pH 2.2, temperature 42 °C, an air supply of 0.4 $m^3/(L \cdot h)$ and stirring speed 65 rpm. The temperature, agitation, pH, and ORP were automatically controlled and monitored online during bio-oxidation process. A daily slurry sample was taken from each tank to analyze Au, S, Fe, and As content in residue and dissolved concentrations of Fe, As and $H_2SO_4$ in solution.

Continuous bio-oxidation procedure: after batch bio-oxidation was completed, city water and gold concentrate were added into a feed tank with 15% slurry density. Subsequently, the slurry from the feed tank was pumped into two first-stage tanks at a flowrate 60 mL/min. The two first-stage tanks' overflow automatically flowed into the second-stage tanks with each tank successively overflowing into another in order from 1# though 4#, and fourth tank of second-stage overflow automatically flowed into the thickener. Lastly, the thickener overflow was neutralized, and the underflow containing bio-oxidation residue was sent to cyanidation after pressurized filtration. A daily slurry sample was also taken from each tank to analyze the Au, S, Fe, and As content in residue and dissolved concentrations of Fe, As and $H_2SO_4$ in solution when continuous bio-oxidation became consistent. The detail flowsheet is shown in Figure 3.

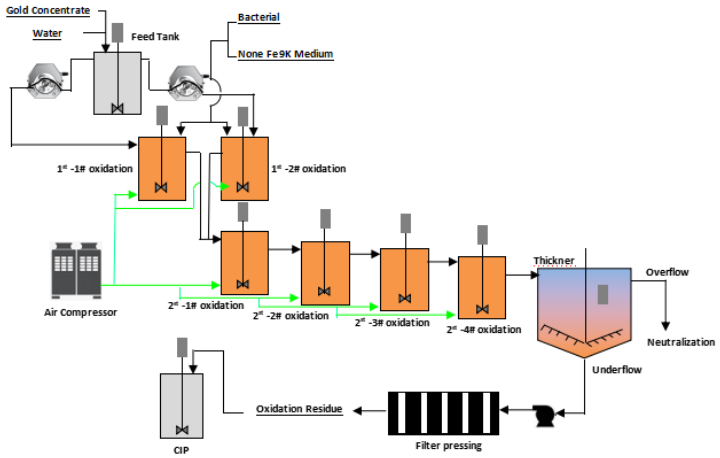


**Figure 3.** Flowsheet of continuous bio-oxidation.

CIL methods: The CIL test was carried out with 30% density and carbon profile of 30 g/L in a 6 L tank, 300 mg/L cyanide was added with quick lime to achieve a stable pH of 10.0. Finally, the residue was sent to assay the gold content after 24 h leaching with a stirring speed of 150 rpm.

DNA extraction, sequencing and microbe statistics:

(1) DNA extraction from ore: a 10 g sample of ore was cleaned with ultra-pure water, the supernatant was collected and transferred into a 5 ml EP tube, and then 2 ml solution A, 200 µLPVP (10%), 200 µLSDS (10%) and 0.5 g sterilized glass beads with 465–600µm were added. The supernatant was transferred into a clean centrifuge tube after gently mixing

and centrifuging at 12,000 rpm for 2 min. After which, 1/10 volume of cold sodium acetate (5M) was added and placed on ice for 10 min, then centrifuged at 12,000 rpm for 5 min. The DNA was extracted using a DNA purification kit (Promega Inc., Madison, WI, USA) and stored at −20 °C for further experiments.

(2) DNA extraction from solution: a 5 L sample of microbe solution was prefiltered by a 1.6 μm membrane to remove coarse particles, and then the microbes were collected using a 0.22 μm filter membrane. The filter membrane was cut into small pieces and the DNA was extracted from these pieces using DNEasy PowerMax Soil Kit (Qiagen, Hilden, Germany). The extracted DNA was stored at −20 °C for further experiments.

(3) 16SrRNA sequencing: the 515FB (5′-GTGYCAGCMGCCGCGGTAA-3′)/926R (5′-CCGYCAATTYMTTTRAGTTT-3′) paired primers were designed to target the V4-V5 hypervariable regions of the 16SrRNA gene in DNA samples. The above-paired primers, KAPA thermally initiated high-fidelity enzyme (KK2602) and sample DNA solution were amplified in a 50 μL system. The PCR program initiated at 3 min at 95 °C, followed by 30 cycles of 20 s at 98 °C, 15 s at 55 °C, 15 s at 72 °C, and a final cycle of 72 °C for 1 min. PCR products were analyzed by 2% agarose gel electrophoresis and, where necessary, purified using Omega PCR purification kit (D2500-02). The DNA concentrations of PCR products were measured using Qubit. After quality control, the addition of A tail at 3′ end, adapter linkage, gel extraction, amplification, and normalization of the DNA library, amplicons were generated, followed by MiSeq sequencing (2 × 250 bp, 40,000 reads per sample).

(4) Real-time PCR procedure: using SYBR Green I kit (Qiagen), 3.125 pole 27F-AT. F384R, L. F402R, S.T424R, F.A57F and F.A460R were added to each reaction system, and 2.34 pmol universal primer was added. The extracted DNA was diluted 100 times with dd$H_2O$ as a template for PCR reaction and then amplified on the PCR in terms of procedure (95 °C at one cycle for 5 min, 95 °C at 40 cycles for 30 s, 60 °C at 40 cycles for 30 s). The TC value (threshold cycle) obtained was compared with the standard curve to obtain the number of each microbe species.

### *2.4. Analytical Method*

The elemental composition of the minerals were measured using atomic absorption spectroscopy (AAS, ICE3400, Thermo Fisher, Waltham, MA, USA) and ICP-MS (XSERIES2, Thermo Fisher, Waltham, MA, USA). The mineralogical contents were measured using mineral liberation analyzer (MLA, MLA650, FEI, Hillsboro, OR, USA) and SEM (Quanta 650, FEI, Hillsboro, OR, USA). The frequency and quantity of microorganisms were analyzed by MiSeq sequencer (Illumina, San Diego, CA, USA) and Rotor-Gene 6000, respectively.

## 3. Results and Discussion

### *3.1. Removal Rate and Kinetics by Different Bio-Oxidation Methods*

As shown in Figure 4a, the removal rates of S and Fe linearly increased by the rate formula $R_S$ = 6.44t−4.07 ($R^2$ = 0.981) and $R_{Fe}$ = 8.05t−14.35 ($R^2$ = 0.967) respectively, during the batch bio-oxidation process, and the removal rate of As increased according to the curves of second-order formula $R_{As} = -0.77t^2 + 19.19t - 20.83$ ($R^2$ = 0.978). Figure 4b shows that the removal rate of the S, Fe and As during the continuous bio-oxidation process had the same trends compared to batch bio-oxidation process with the rate formulas $R^*_S$ = 12.02t−1.30 ($R^2$ = 0.998), $R^*_{Fe}$ = 12.17t + 1.34 ($R^2$ = 0.988) and $R^*_{As} = 2.33t^2 + 28.27t + 1.77$ ($R^2$ = 0.986), respectively. Continuous bio-oxidation yielded removal rates of 83.83%S, 83.5%Fe, 92.58%As, and a corresponding 94.71% gold recovery in 7 days; it requires 13 days to achieve similar results via the batch bio-oxidation process. As illustrated in Figure 4c,d, the gold recovery linearly increased as the S removal rate increased. The linear fit of gold recovery for batch and continuous bio-oxidation is $R_{Au} = 0.37R_s + 63.76$ ($R^2$ = 0.97) and $R_{Au} = 0.41R^*_s + 59.76$ ($R^2$ = 0.99), respectively. Therefore, liberating the enclosed gold in pyrite and arsenopyrite by bio-oxidation is the best option to improve gold recovery. The S, Fe and As kinetic formula of batch bio-oxidation is $V_S$ = 6.44%, $V_{Fe}$ = 8.05%, $V_{As} = -1.54t + 19.19$, respectively, which is the derivative of their removal

rates with respect to their individual bio-oxidation time (Figure 4a,b). The continuous bio-oxidation removal rates were $V^*_S$ = 12.02%, $V^*_{Fe}$ = 12.17% and $V^*_{As}$ = −4.46t +28.27, respectively. The removal rates of S and Fe were constant at 12.02% and 12.17% per day by continuous bio-oxidation, respectively, which were 86.64% and 51.18% higher than the constant 6.44% and 8.05% yielded by batch bio-oxidation, respectively. When the bio-oxidation time was less than three days, the removal rate of As during continuous bio-oxidation was significantly higher than batch bio-oxidation ($V^*_{As} > V_{As}$), a relationship that was inversely proportional after 3 days. The As was almost completely removed after 6.3 days in both the bio-oxidation processes.

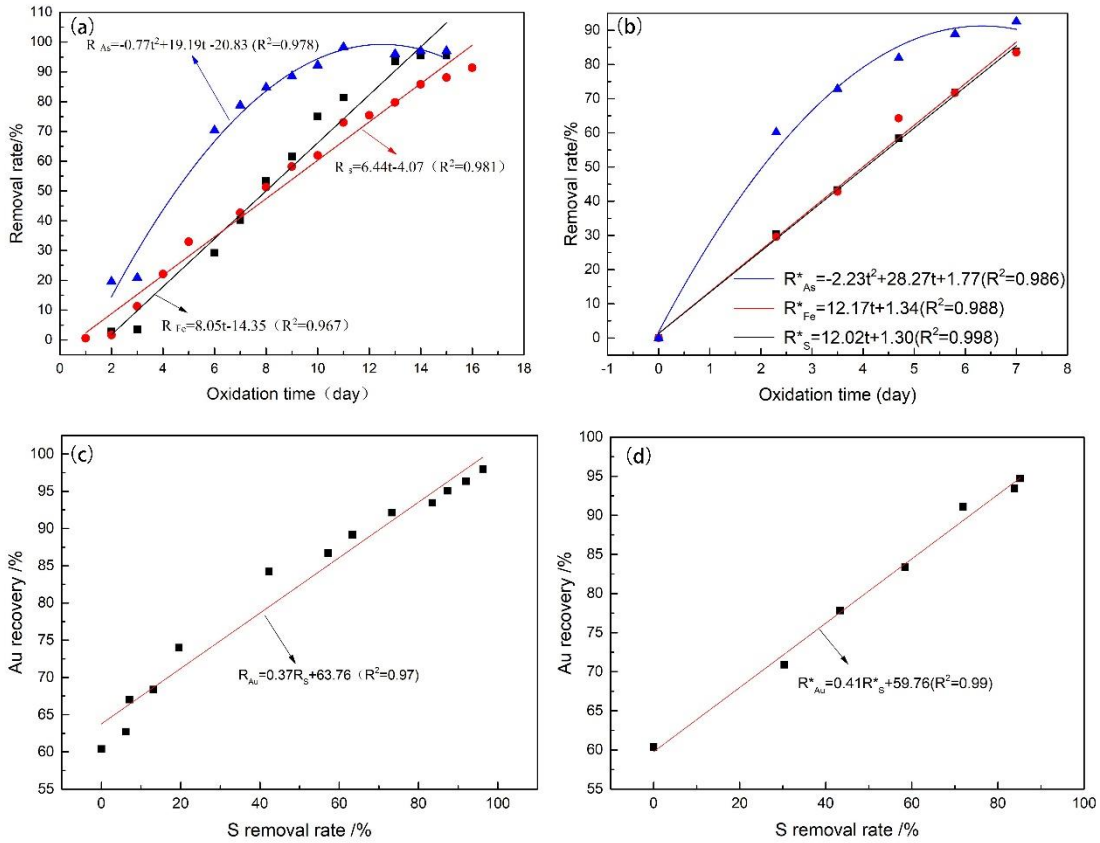


**Figure 4.** S, Fe, As removal rate and gold recovery: (**a**) S, Fe, As removal rate by batch bio-oxidation, (**b**) S, Fe, As removal rate by continuous bio-oxidation, (**c**) relationship of gold recovery and sulfur removal rate by batch bio-oxidation, (**d**) relationship of gold recovery and sulfur removal rate by continuous bio-oxidation.

Batty and Rorke [24] demonstrated that the exact extent of dissolution was achieved with half the leach time in the continuous system as compared to the batch leach test on the same chalcopyrite concentrate. However, the compared study on removal rates and kinetics of S, Fe, As by high sulfur and arsenic refractory concentrate batch and continuous bio-oxidation has not been reported.

The refractory gold concentrate particle size used in this study was 90%−0.074 mm, and the influence of concentrate particle size has been investigated before this study. The results showed that the particle size had insignificant effect on batch and continuous bio-oxidation process. Since most of the electrum size enclosed by minerals was as fine as −10 μm, the minimum grinding size to be milled by rod and ball was coarser than the enclosed electrum in minerals.

### *3.2. Influence Factors on Bio-Oxidation Kinetics*

As shown in Figure 5, the dissolved concentration of Fe, $H_2SO_4$, As and microbe population increased stepwise and remained constant in continuous bio-oxidation. Fe,

$H_2SO_4$ and microbes increased linearly and As increased via second-order equation in the batch bio-oxidation process with the concentration formula $C_{Fe}$ = 2.62t −1.58 ($R^2$ = 0.99), $C_{H2SO4}$ = 2.84t−2.38 ($R^2$ = 0.99) and $C_{As}$ = −0.025$t^2$ + 0.53t−0.33 ($R^2$ = 0.95). Fe, $H_2SO_4$, As concentrations and microbe populations were 31.94 g/L, 33.53 g/L, 2.19 g/L and 2.57 × $10^8$/mL in solution, respectively, achieved by continuous bio-oxidation in 7 days, as opposed to 13 days via batch bio-oxidation for similar concentrations. This corresponded with the removal rates of S, Fe and As observed in Section 3.1 between batch and continuous bio-oxidation. Fe, $H_2SO_4$, As and microbes increased by 6.77 g/L, 7.47 g/L, 0.10 g/L and 1.08 × $10^3$/mL, respectively, higher than batch bio-oxidation. The population of microbes and dissolved concentration in the continuous bio-oxidation process was significantly higher than in the batch bio-oxidation process.

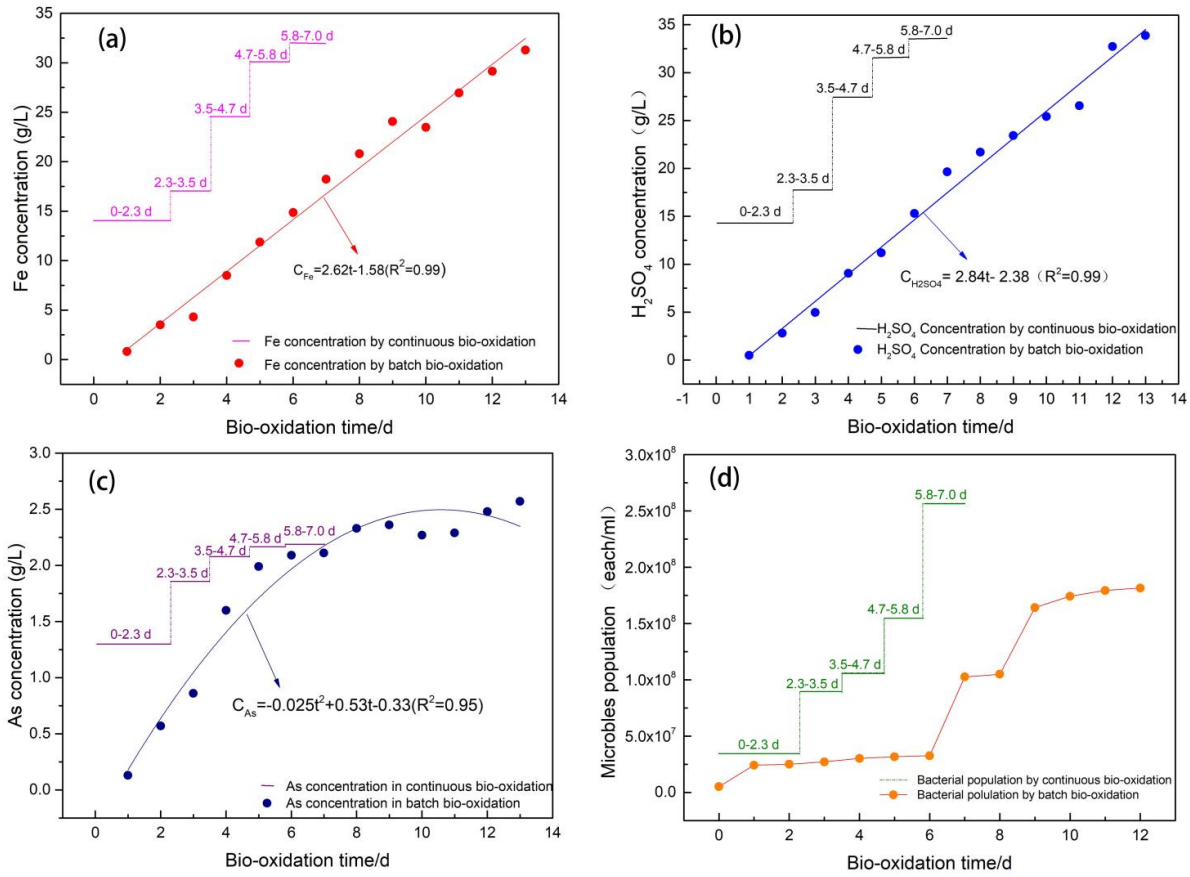


**Figure 5.** Ion concentrations and microbe populations in batch and continuous bio-oxidation, (**a**) Fe concentration, (**b**) $H_2SO_4$ concentration, (**c**) As concentration, (**d**) microbe populations.

Bio-oxidation, chemical oxidation and electrochemical etch reaction accompanied the sulfide bio-oxidation process of refractory gold concentrate [25–27]. The pyrite and arsenopyrite were oxidized into sulfate and metal ions by direct contact between microbes and sulfide minerals in the presence of oxygen as shown in reactions (1) and (2). The kinetics of continuous bio-oxidation was higher than the batch bio-oxidation process because of a greater microbe concentration in the continuous bio-oxidation process as opposed to the batch bio-oxidation process as shown in Figure 5d. This process provided a continuous, dynamic and open system which was beneficial for microbe growth and oxidation in the continuous bio-oxidation process. Hence, increasing the microbe population stepwise and maintaining the equilibrium at each step (Figure 5d). This was the key reason for a higher microbe population as compared to a closed independent system; which was adverse to microbe growth and oxidation in batch bio-oxidation process. Lastly, the kinetics and

relative sulfide acid concentration in the continuous bio-oxidation process is much higher than batch bio-oxidation based on reactions (1) and (2).

The $Fe^{2+}$ and $As^{3+}$ generated by the direct bio-oxidation of pyrite and arsenopyrite were oxidized into $Fe^{3+}$ and $As^{5+}$ by indirect bio-oxidation as shown in reactions (3) and (4), respectively. Pyrite and arsenopyrite were oxidized by $Fe^{3+}$ [28] into $Fe^{2+}$ and $As^{3+}$ according to reactions (5) and (6), respectively. $Fe^{2+}$ and $As^{3+}$ were subsequently oxidized into $Fe^{3+}$ and $As^{5+}$ by direct microbe bio-oxidation reactions (3) and (4), respectively. The oxidation of Fe and As is the redox cycle of $Fe^{2+}$ ($As^{3+}$) and $Fe^{3+}$ ($As^{5+}$) in the mineral and solution interface [29]. The continuous bio-oxidation final kinetics were faster than batch bio-oxidation since its concentration of $Fe^{3+}$ was higher (Figure 5a,c). The higher concentration of $Fe^{3+}$ and $H_2SO_4$ were beneficial to the chemical oxidation of pyrite [30,31]. The kinetics of chemical reactions of (5) and (6) by continuous bio-oxidation were higher than that of the batch bio-oxidation process as $Fe^{3+}$ concentration in the continuous bio-oxidation process increased stepwise and was higher than batch bio-oxidation, which increased linearly.

$$2FeS_2 + 7O_2 + 2H_2O \xrightarrow{\substack{Acidithiobacillus,\ Leptospirillum \\ Ferroplasm,\ Sulfobacillus,\ etc}} 2Fe^{2+} + 4{SO_4}^{2-} + 4H^+ \quad (1)$$

$$4FeAsS + 13O_2 + 6H_2O \xrightarrow{\substack{Acidithiobacillus,\ Leptospirillum \\ Ferroplasm,\ Sulfobacillus,\ etc}} 4Fe^{2+} + 4{SO_4}^{2-} + 12H^+ + 4{AsO_4}^{2-} \quad (2)$$

$$4Fe^{2+} + O_2 + 4H^+ \xrightarrow{\substack{Acidithiobacillus,\ Leptospirillum \\ Ferroplasm,\ etc}} 4Fe^{3+} + 2H_2O \quad (3)$$

$$2As^{3+} + O_2 + 4H^+ \xrightarrow{\substack{Acidithiobacillus,\ Leptospirillum \\ Ferroplasm,\ etc}} 2As^{5+} + 2H_2O \quad (4)$$

$$FeS_2 + 2Fe^{3+} = 3Fe^{2+} + 2S^0 \quad (5)$$

$$FeAsS + 7Fe^{3+} + 4H_2O = {H_2AsO_4}^- + 8Fe^{2+} + S^0 + 6H^+ \quad (6)$$

As is evident from Figure 6, the pH of continuous and batch bio-oxidation decreased stepwise and linearly, respectively, in comparison with ORP which increased stepwise and linearly, respectively. The pH (0.5) and ORP (614.1 mV, vs. Ag/AgCl) was achieved in 7 days by continuous bio-oxidation while batch bio-oxidation took 13 days and 10 days, respectively. The ORP and $Fe^{3+}/Fe^{2+}$ relationship can be expressed by the Nernst equation [32] $E_h = E^0 + 0.059\lg \frac{m_{Fe^{3+}}}{m_{Fe^{2+}}}$ during bio-oxidation process, with higher ORP being more beneficial to the kinetics of pyrite and arsenopyrite.

### 3.3. Microbe Culture and Population

As illustrated in Figure 7a, there were 26 genera with a relative frequency greater than 0.2% in the microbes sampled from waste acid residue of Zijinshan Gold and Copper mine. Among these, eight genera's relative frequencies were greater than 2%: *Acidithiobacillus* 37.45%, *Sulfobacillus* 15.79%, *Ferroplasma* 11.54%, *Leptosirillum* 10.34%, *Acidiferrobacter* 7.89%, *Acidiplasma* 2.75%, *Raoultella* 2.28%, *Acidiphilium* 2.33%. There were 19 genera with a relative frequency greater than 0.2% in the microbes sampled from AMD of Zijinshan Gold and Copper mine. Among these, six genera's relative frequencies were greater than 2%: *Leptospirillum* 59.01%, unclassified *Karchae* 19.89%, *A-plasma* 8.90%, *Sulfobacillus*

2.36%, *Ferroplasma* 2.17%, *Cuniculiplasma* 2.15%. The microbe cultures in waste acid residue are seven and two more than in AMD for relative frequency greater than 0.2% and 2%, respectively. Moderately thermophilic microbes such as *Acidithiobacillus*, *Acidiphilium* and more moderate thermophilic microbes such as *Leptospirillum*, *Ferroplasma*, *Acidiferrobacter*, *Sulfobacillus* are dominated by iron-oxidizing and sulfur-oxidizing microbes.

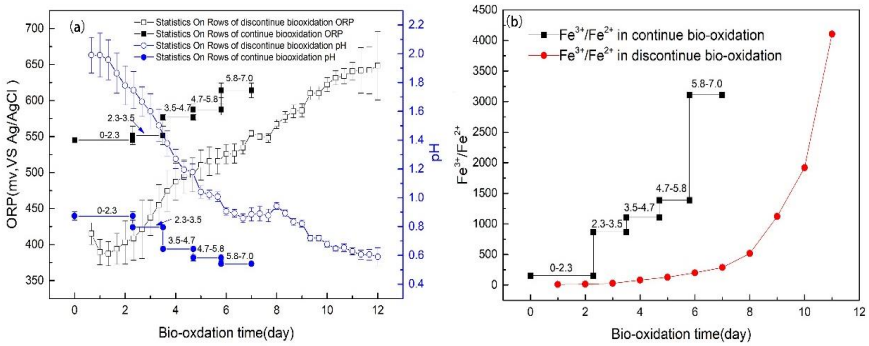


**Figure 6.** ORP and pH trend during continuous and batch bio-oxidation process.

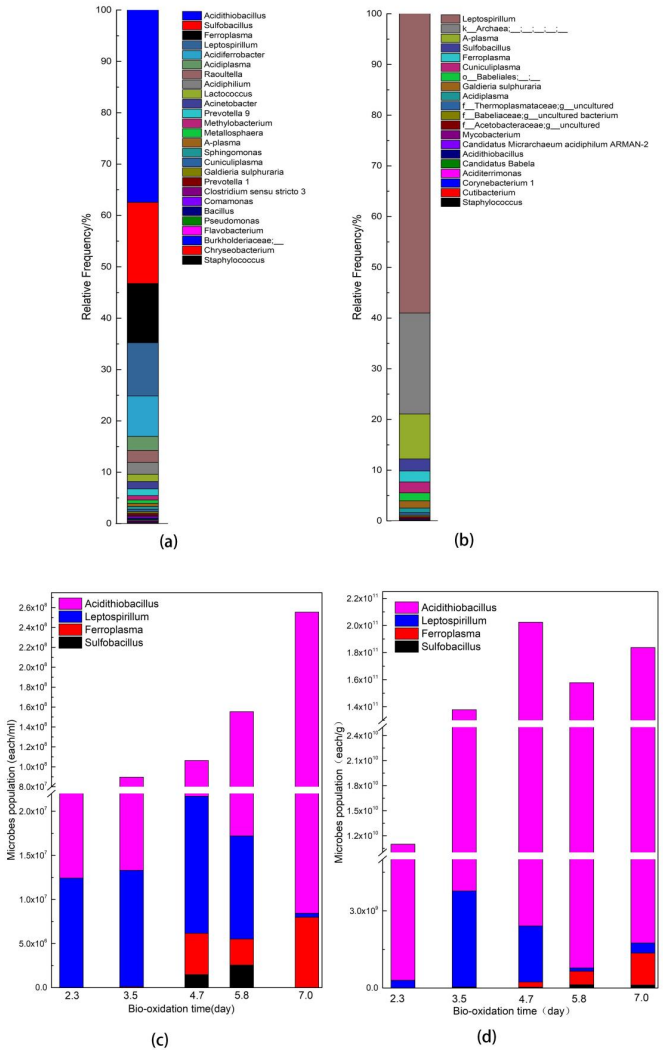


**Figure 7.** Microbe culture, frequency and population. (**a**) relative frequency of microbes from Zijinshan Gold and Copper mine waste acid residue, (**b**) relative frequency of microbes from Zijinshan Gold and Copper mine AMD, (**c**) microbe populations in solution during continuous bio-oxidation process, (**d**) microbe populations in solids during continuous bio-oxidation process.

Archaea such as *Ferroplasma* have been utilized with bacteria for bio-oxidation, but Archaea are historically overshadowed by bacteria in terms of public awareness. As shown in Figure 7a,b, there were five and seven archaea cultures in waste acid residues and AMD with the total frequency of 15.96% and 35.26%, respectively. The five archaea in waste acid residue were *Ferroplasma*, *Acidiplasma*, *Metallosphaera*, *A-plasma* and *cuniculiplasma* of which four are in the subdivision of *Euryarchaeota* and the fifth one *Metallosphaera,* is in the subdivision of Crenarchaeota. For seven archaea in AMD, these five, A-plasma, *Ferroplasma, Cuniculiplasma, Acidiplasma, f_Thermoplasmataceae; g*_uncultured were in the subdivision of Euryarchaeota, *Candidatus Micrarchaeum acidiphilum ARMAN-2* was in the subdivision of Diapherotrites and K-Archaea was uncultured even in Phylum level. Most studies on archaea are only for the explanation of their adaptability, and few were conducted on bio-oxidation since archaea can hardly be separated and cultured in the laboratory. The main reason being its extreme environmental growth requirements and the special structure of different archaea. Archaea are more active and competitive in extreme environments such as highly acidic, an-aerobic, saline and high temperature when compared to bacterial. However, further mechanism and application potential for the mining industry need to be investigated.

The greatest relative frequency of microbes were the *Acidithiobacillus*, *Leptospirillum*, *Ferroplasma* and *Sulfobacillus*. Their relative populations were $1.37 \times 10^{11}$/g, $1.35 \times 10^{9}$/g, $3.95 \times 10^{8}$/g and $6.28 \times 10^{7}$/g, respectively (Figure 7b), compared with $1.14 \times 10^{8}$/mL, $1.07 \times 10^{7}$/mL, $3.14 \times 10^{6}$/mL, and $8.13 \times 10^{5}$/mL in solution (Figure 7c). The average population of these four genera in solids was $1.08 \times 10^{3}$ higher than in solution during the bio-oxidation process. This can be attributed to *Acidithiobacillus*, *Leptospirillum*, *Ferroplasma* and *Sulfobacillus* microbes obtaining energy growth and oxidation by adhering to the solid surface of pyrite and arsenopyrite, forming extracellular polymer EPS between the ore surface and the solution [33,34]. The main function of bacteria adhering to the sulfur mineral surface in the form of EPS is oxide $[Fe_2]^{2+}$ and $S^{2-}$ of pyrite into $Fe^{2+}$ and $SO_4{}^{2-}$ (reaction (1)) during the bio-oxidation of refractory gold concentrate. $[FeAs]^{2+}$, $S^{2-}$ of arsenopyrite was oxidized into $Fe^{2+}$, $SO_4{}^{2-}$ and $AsO_4{}^{2-}$ (reaction (2)), respectively. Thus, causing the population of microbes to be much higher compared to the population of microbes in highly concentrated $H_2SO_4$ and arsenic ion solution (Figure 5b,c) without the protection of EPS.

$Fe^{2+}$ and $As^{3+}$ was oxidized into $Fe^{3+}$ and $As^{5+}$ by *Acidithiobacillus*, *Leptospirillum* and *Ferroplasma* via direct bio-oxidation in solution as shown in reactions (3) and (4) of Section 3.2. $SO_3{}^{3-}$ can be oxidized into $SO_4{}^{2-}$ by *Acidithiobacillus* and *Sulfobacillus* in solution. The multi-microbes used in this study had high bio-oxidation activity in pH 0.5 and arsenic solution (Figure 7a) since some archaea co-existed and co-contributed where the pH was much lower than the currently reported pH 1.2–1.6 in the bio-oxidation process [11,35].

The depth and numbers of microbe etching pits increased with the bio-oxidation processes, as shown in Figure 8. The surface area increased with the depth and number of etching pits, thus, a larger surface area was available for more microbe bio-oxidation on the pyrite mineral's surface. Therefore, the population of microbes increased within 4.7 days via bio-oxidation (Figure 7c). However, the population of microbes in the solids began to decrease (Figure 7d) because the core contraction of pyrite and surface area decreased gradually after 4.7 days. Mustin et al. [36] reported that the surface area of pyrite before and after biological oxidation was 1.1 and 1.6 $m^2$/g, respectively.

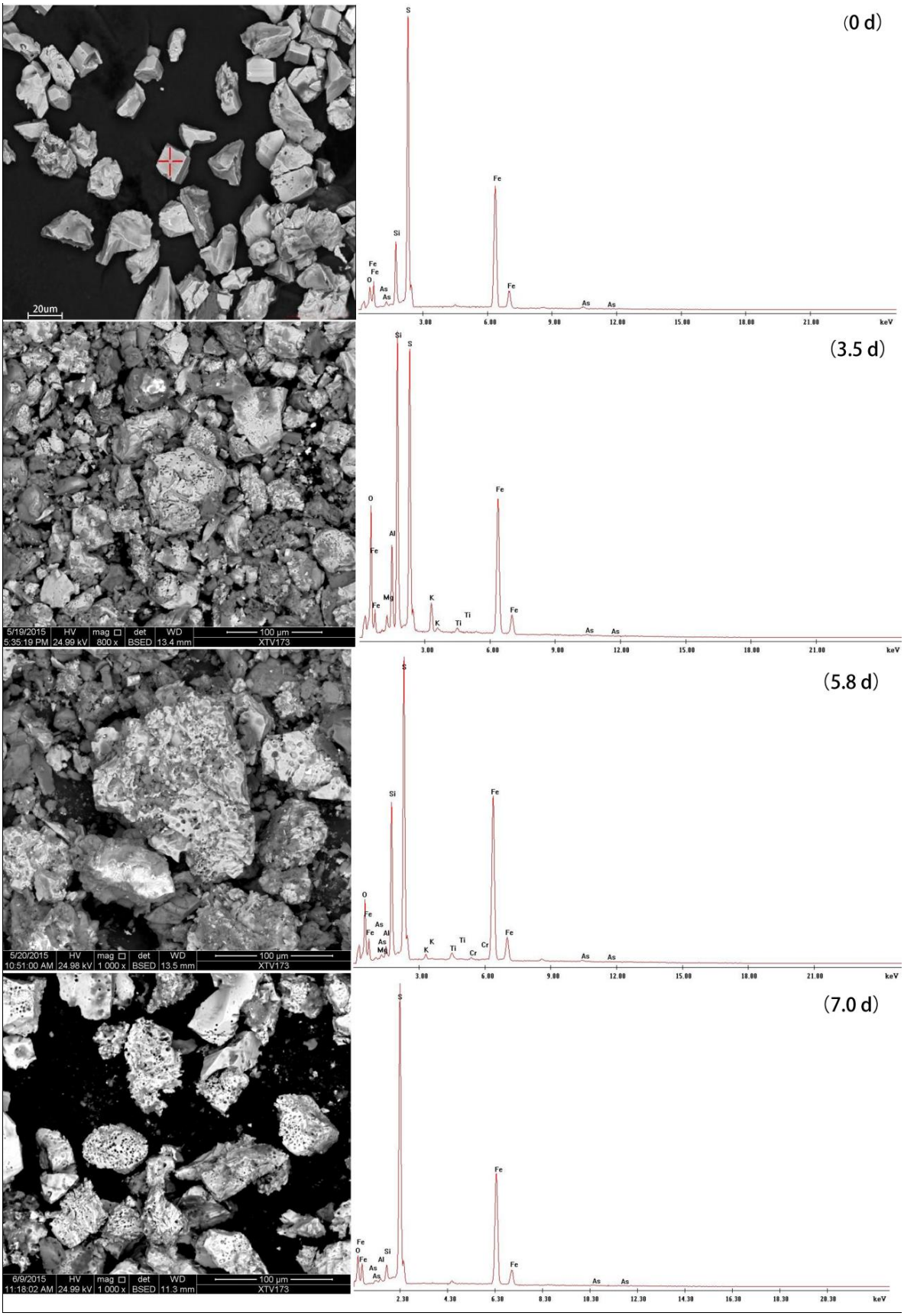


**Figure 8.** SEM and EDX of residue during continuous bio-oxidation procedure.

The particle area was decreasing with the bio-oxidation progressing on the refractory gold concentrate since the S, Fe and As in pyrite and arsenopyrite was bio-oxidized into solution as $SO_4^{2-}$, $Fe^{3+}$, $As^{5+}$ and $As^{3+}$, etc. The residue particle sizes after 2.3 days, 4.7 days, 5.8 days and 7.0 days bio-oxidation were 94.57%−0.074 mm, 96.39%−0.074 mm, 80.52%−0.045 mm and 87.35%−0.045 mm, respectively, compared to 90% -0.074 mm of concentrate. The residue final cyanidation gold recovery of free gold; gold enclosed in sulfide; gold enclosed in oxide and sulfate and gold enclosed in quartz was 98.32%, 93.46%, 98.46% and 26.52%, respectively. Gold enclosed in quartz only accounted for 0.41% of the total gold, and the small amount of gold recovered from quartz was partly-enclosed with quartz which could be leached by cyanide. Bio-oxidation, pressure oxygen oxidation and roasting technology all are inactive on quartz.

## 4. Conclusions

In this study, it was found that bio-oxidation methods were one of the main influencing factors on kinetics. The results of the relationship of S, Fe and As removal with gold recovery by different bio-oxidation methods showed that gold recovery from batch and continuous bio-oxidation linearly increased as the sulfur removal rate increased, and in terms of the formula were $R_{Au}$ = 0.37Rs + 63.76 ($R^2$ = 0.97) and $R^*_{Au}$ = 0.41$R^*$s + 59.76 ($R^2$ = 0.99), respectively. The removal rates of S, Fe and relative gold recovery linearly increased when compared to the second-order equation increase of the As removal rate in both batch and continuous bio-oxidation processes. S and Fe removal kinetics were 12.02% and 12.17% by continuous bio-oxidation which were 86.64 and 51.18% higher in comparison to batch bio-oxidation removal kinetics. The 83.83% S, 83.5% Fe, 92.58% As removal rates and corresponding 94.71% gold recovery was achieved within 7 days by continuous bio-oxidation as opposed to the 13 days taken by batch bio-oxidation.

The investigation of the dissolved ions concentration during the bio-oxidation process showed that the higher kinetics of continuous bio-oxidation resulted from a stepwise increase in microbe growth, larger populations and higher dissolved $Fe^{3+}$ and $H_2SO_4$ concentrations compared to a linear increase by batch bio-oxidation. The dissolved concentration of 31.94 g/L Fe, 33.53 g/L $H_2SO_4$ and 2.19 g/L As was achieved in 7 days by continuous bio-oxidation as opposed to 13 days in batch bio-oxidation.

The 16sRNA sequencing results showed that there are 26 different microbes in the initial residue and 7 more than AMD at genus level. PCR test showed that the four most popular microbes were *Acidithiobacillus*, *Leptospirillum*, *Ferroplasma* and *Sulfobacillus*, and their average population in continuous bio-oxidation residue was 1.08E+03 higher than in solution. During the bio-oxidation process, the microbe population crash time was 4.7 days, shifting from increasing to decreasing. Multi-microbe strains had high activity and performance in lower pH 0.5–0.9 environment, compared to reported pH 1.2–1.6, since some archaea co-exist and co-contribute.

**Author Contributions:** Conceptualization and supervision, T.-Z.Y.; investigation and writing, Z.-S.H. All authors have read and agreed to the published version of the manuscript.

**Funding:** The research was supported by the Natural Science Foundation of China (No. 51874101, granted on 2 January 2019).

**Data Availability Statement:** Not applicable.

**Acknowledgments:** The authors give a special thanks to Zijin Mining Group Co., Ltd. (Xiamen, China) and the State Key Laboratory of Comprehensive Utilization of Low-Grade Refractory Gold Ore.

**Conflicts of Interest:** The authors declare no conflict of interest.

## References


1. Yang, H.-Y.; Liu, Q.; Song, X.-L.; Dong, J.-K. Research status of carbonaceous matter in carbonaceous gold ores and bio-oxidation pretreatment. *Trans. Nonferrous Met. Soc. China* **2013**, *23*, 3405–3411. [CrossRef]
2. Konadu, K.T.; Mendoza, D.M.; Huddy, R.J.; Harrison, S.T.; Kaneta, T.; Sasaki, K. Biological pretreatment of carbonaceous matter in double refractory gold ores: A review and some future considerations. *Hydrometallurgy* **2020**, *196*, 105434. [CrossRef]
3. Qin, H.; Guo, X.; Tian, Q.; Yu, D.; Zhang, L. Recovery of gold from sulfide refractory gold ore: Oxidation roasting pretreatment and gold extraction. *Miner. Eng.* **2021**, *164*, 106822. [CrossRef]
4. Zhang, D.C.; Xiao, Q.K.; Liu, W.F.; Chen, L.; Yang, T.Z.; Liu, Y.N. Acid leaching decarbonization and following pressure oxi-dation of carbonic refractory gold ore. *J. Cent. South Univ.* **2016**, *23*, 1584–1590. [CrossRef]
5. Marsden, J.O.; House, C.I. *The Chemistry of Gold Extraction*, 2nd ed.; SME: Littleton, CO, USA, 2006; pp. 190–200.
6. Li, Q.; Li, D.; Qian, F. Pre-oxidation of high-sulfur and high-arsenic refractory gold concentrate by ozone and ferric ions in acidic media. *Hydrometallurgy* **2009**, *97*, 61–66. [CrossRef]
7. Wang, Q.; Hu, X.; Zi, F.T.; Yang, P.; Chen, Y.L.; Chen, S.L. Environmentally friendly extraction of gold from refractory concen-trate using a copper-ethylenediamine-thiosulfate solution. *J. Clean. Prod.* **2019**, *214*, 860–872. [CrossRef]
8. Mubarok, M.Z.; Winarko, R.; Chaerun, S.K.; Rizki, I.N.; Ichlas, Z.T. Improving gold recovery from refractory gold ores through biooxidation using iron-sulfur-oxidizing/sulfur-oxidizing mixotrophic bacteria. *Hydrometallurgy* **2017**, *168*, 69–75. [CrossRef]
9. Ahn, J.; Wu, J.J.; Ahn, J.; Lee, J. Comparative investigations on sulfidic gold ore processing: A novel biooxidation process option. *Miner. Eng.* **2019**, *140*, 105864. [CrossRef]
10. Brierley, C.L.; Brierley, J.A. Progress in bioleaching: Part B: Applications of microbial processes by the minerals industries. *Appl. Microbiol. Biotechnol.* **2013**, *97*, 7543–7552. [CrossRef]
11. Van Aswegen, P.C.; Niekerk, J.V.; Olivier, W. *Biomining*; Johnson, D.B., Ed.; Springer: Berlin, Germany, 2007; pp. 1–33.
12. Mahmoud, A.; Cézac, P.; Hoadley, A.; Contamine, F.; D'Hugues, P. A review of sulfide minerals microbially assisted leaching in stirred tank reactors. *Int. Biodeterior. Biodegrad.* **2017**, *119*, 118–146. [CrossRef]
13. Zhang, L.; Qiu, G.-Z.; Hu, Y.-H.; Sun, X.-J.; Li, J.-H.; Gu, G.-H. Bioleaching of pyrite by A. ferrooxidans and L. ferriphilum. *Trans. Nonferrous Met. Soc. China* **2008**, *18*, 1415–1420. [CrossRef]
14. Loi, G.; Rossi, A.; Trois, P.; Rossi, G. Continuous revolving barrel bioreactor tailored to the bioleaching microorganisms. *Min. Met. Explor.* **2006**, *23*, 196–202. [CrossRef]
15. Climo, M.; Watling, H.; Van Bronswijk, W. Biooxidation as pre-treatment for a telluride-rich refractory gold concentrate. *Miner. Eng.* **2000**, *13*, 1219–1229. [CrossRef]
16. Hong, J.; Silva, R.A.; Park, J.; Lee, E.; Park, J.; Kim, H. Adaptation of a mixed culture of acidophiles for a tank biooxidation of refractory gold concentrates containing a high concentration of arsenic. *J. Biosci. Bioeng.* **2016**, *121*, 536–542. [CrossRef]
17. Zhang, M.-J.; Jiang, C.-Y.; You, X.-Y.; Liu, S.-J. Construction and application of an expression vector from the new plasmid pLAtc1 of Acidithiobacillus caldus. *Appl. Microbiol. Biotechnol.* **2014**, *98*, 4083–4094. [CrossRef] [PubMed]
18. Peng, J.B.; Yan, W.M.; Bao, X.Z. Expression of heterogenous arsenic resistance Ggenes in the obligately autotrophic biomining bacterium Thiobacillus-ferrooxidans. *Appl. Environ. Microbiol.* **1994**, *60*, 2653–2656. [CrossRef]
19. Kaksonen, A.H.; Boxall, N.J.; Gumulya, Y.; Khaleque, H.N.; Morris, C.; Bohu, T.; Cheng, K.Y.; Usher, K.M.; Lakaniemi, A.M. Re-cent progress in bio-hydrometallurgy and microbial characterization. *Hydrometallurgy* **2018**, *180*, 7–25. [CrossRef]
20. Rawlings, D. The molecular genetics of Thiobacillus ferrooxidans and other mesophilic, acidophilic, chemolithotrophic, iron- or sulfur-oxidizing bacteria. *Hydrometallurgy* **2001**, *59*, 187–201. [CrossRef]
21. Chandraprabh, M.N.; Modak, J.M.; Natarajan, K.A.; Raichur, A.M. Strategies for efficient start-up of continuous biooxidation process for refractory gold ores. *Miner. Eng.* **2002**, *15*, 751–753. [CrossRef]
22. Marchevsky, N.; Quiroga, M.B.; Giaveno, A.; Donati, E. Microbial oxidation of refractory gold sulfide concentrate by a native consortium. *Trans. Nonferrous Met. Soc. China* **2017**, *27*, 1143–1149. [CrossRef]
23. Hansford, G.S.; Chapman, J.T. Batch and continuous bio-oxidation kinetics of a refractory gold-bearing pyrite concentrate. *Miner. Eng.* **1992**, *6*, 597–612. [CrossRef]
24. Batty, J.; Rorke, G. Development and commercial demonstration of the BioCOP™ thermophile process. *Hydrometallurgy* **2006**, *83*, 83–89. [CrossRef]
25. Sand, W.; Gehrke, T.; Jozsa, P.G.; Schippers, A. Direct versus indirect bioleaching. *Process Metall.* **1999**, *9*, 27–49. [CrossRef]
26. Tributsch, H. Direct versus indirect bioleaching. *Hydrometallurgy* **2001**, *59*, 177–185. [CrossRef]
27. Gu, G.-H.; Hu, K.-T.; Li, S.-K. Surface characterization of chalcopyrite interacting with Leptospirillum ferriphilum. *Trans. Nonferrous Met. Soc. China* **2014**, *24*, 1898–1904. [CrossRef]
28. Charpentier, D.; Buatier, M.; Jacquot, E.; Gaudin, A.; Wheat, G.C. Conditions and Mechanism for the formation of iron-rich Montmorillonite in deep sea sediments (Costa Rica margin): Coupling high resolution mineralogical characterization and ge-ochemical modeling. *Geochim. Cosmochim. Acta* **2011**, *75*, 1397–1410. [CrossRef]
29. Donati, E.R.; Sand, W. (Eds.) *Microbial Processing of Metal Sulfides*; Springer: Dordrecht, The Netherlands, 2007; pp. 15–30.
30. Zhong, S.P.; Wu, Z.; Huang, Z.S.; Ruan, R.M. Oxidation Kinetics Reaction of Gold-Bearing Pyrite in Sulphuric Acid. *Chin. J. Rare Met.* **2013**, *2*, 295–301.
31. Liu, F.; Shi, J.; Duan, J.; Zhou, L.; Xu, J.; Hao, X.; Fan, W. Significance of jarosite dissolution from the biooxidized pyrite surface on further biooxidation of pyrite. *Hydrometallurgy* **2018**, *176*, 33–41. [CrossRef]

32. Saavedraa, A.; Aguirrea, P.; Gentinaa, J.C. Climbing the hill: The implications of a two-step adaptation on biooxidation of fer-rous ion at high total iron concentrations by At. Ferrooxidans. *Hydrometallurgy* **2020**, *197*, 1–8. [CrossRef]
33. Mangold, S.; Harneit, K.; Rohwerder, T.; Claus, G.; Sand, W. Novel Combination of Atomic Force Microscopy and Epifluorescence Microscopy for Visualization of Leaching Bacteria on Pyrite. *Appl. Environ. Microbiol.* **2008**, *74*, 410–415. [CrossRef]
34. Michel, C.; Bény, C.; Delorme, F.; Poirier, L.; Spolaore, P.; Morin, D.; D'Hugues, P. New protocol for the rapid quantification of exopolysaccharides in continuous culture systems of acidophilic bioleaching bacteria. *Appl. Microbiol. Biotechnol.* **2009**, *82*, 371–378. [CrossRef] [PubMed]
35. Coram, N.J.; Rawlings, D.E. Molecular relationship between two groups of the genus Leptospirillum and the finding that Leptospirillum ferriphilumsp. nov. dominates South African commercial biooxidation tanks that operate at 40 °C. *Appl. Environ. Microbiol.* **2002**, *68*, 838–845. [CrossRef] [PubMed]
36. Mustin, C.; Berthelin, J.; Marion, P.; de Donato, P. Corrosion and electrochemical oxidation of a pyrite by Thiobacillus ferroox-idans. *Appl. Environ. Microbiol.* **1992**, *58*, 1175–1182. [CrossRef] [PubMed]